American Mineralogist, Volume 69, pages 771–776, 1984

Crystal structure and optical spectroscopy (300 to 2200 nm) of $CaCrSi_4O_{10}$

HOWARD L. BELSKY

Department of Earth and Space Sciences
State University of New York, Stony Brook, New York 11794

GEORGE R. ROSSMAN

Division of Geological and Planetary Sciences
California Institute of Technology, Pasadena, California 91109

CHARLES T. PREWITT

Department of Earth and Space Sciences
State University of New York, Stony Brook, New York 11794

AND TIBOR GASPARIK

Department of Geophysical Sciences
The University of Chicago, Chicago, Illinois 60637

Abstract

Crystals of $CaCr^{2+}Si_4O_{10}$ were synthesized at 1 atm and 1400–1350°C in a closed system with $fO_2 < 10^{-16}$ bar. $CaCrSi_4O_{10}$ crystallizes in the space group $P4/ncc$ with **a** = 7.378(5)Å and **c** = 15.119(2)Å. The structure was refined to $R = 0.026$ ($R_w = 0.031$) based on 546 reflections. $CaCrSi_4O_{10}$ is a structural analog of gillespite and other $ABSi_4O_{10}$ compounds, and although not itself a mineral, has been shown to exhibit structural and compression properties nearly identical to those of gillespite. The most interesting aspects of the structure are the square-planar coordination of Cr^{2+}, and the Si–Ol–Si bond angle of 176.8°. Apparently, Cr^{2+} is stable in the gillespite structure because it is readily accepted into the square-planar site, in contrast to other Cr^{2+} compounds that are distorted from type-structures as a result of the Jahn–Teller effect in Cr^{2+}. The optical absorption spectrum of $CaCrSi_4O_{10}$ has bands at 511 and 670 nm polarized $\perp$ **c** and at 453 nm $\parallel$ **c**, with all absorption occuring only through vibronic coupling. Diamond cell experiments indicate that $CaCrSi_4O_{10}$ remains tetragonal to at least 50 kbar, with compression behavior identical to that of gillespite.

Introduction

Until recently, minerals containing divalent chromium were virtually unknown. Cr^{2+} was first observed by Haggerty et al. (1970) in lunar minerals, and by Meyer and Boyd (1972) in terrestrial olivines included in diamonds from kimberlites. The presence of Cr^{2+} in meteorites was established by Keil and Brett (1973) in the mineral later named heideite [$(Fe,Cr)_{1+x}(Ti,Fe)_2S_4$], and is implied by the formula for brezinaite, Cr_3S_4 (Bunch and Fuchs, 1969). No known terrestrial mineral contains divalent chromium as an essential element. Nevertheless, the presence of small amounts of Cr^{2+} in lunar, and possibly mantle phases, suggests that the mineral chemistry of divalent chromium is a topic worthy of investigation. Furthermore, the electronic configuration of divalent chromium and the resulting Jahn–Teller effect make Cr^{2+} interesting from a purely crystal-chemical viewpoint.

Gasparik (1981) synthesized several Cr^{2+}-bearing phases in the system CaO–MgO–Cr^0–Cr_2O_3–SiO_2, including the new compound $CaCrSi_4O_{10}$. The crystals of $CaCrSi_4O_{10}$ used in this study were synthesized at 1 atm in an evacuated and closed silica glass tube by cooling from 1400°C to 1350°C in 24 hours. The starting material was a mechanical mix of 3.1 moles of SiO_2, 1.0 $CaSiO_3$, 0.33 Cr_2O_3, and 0.4 Cr^0. An excess of chromium metal kept the oxygen fugacity below the Cr^0–Cr_2O_3 buffer, approximately 10^{-16} bar at 1300°C. The run produced compact aggregates of subhedral plates separated by small amounts of blue interstitial glass. The crystals are pink to

0003–004X/84/0708–0771$02.00

magenta in color, and show good cleavage perpendicular to the [001] direction.

The $ABSi_4O_{10}$ stoichiometry of $CaCrSi_4O_{10}$, coupled with its pronounced cleavage, suggested a relationship to gillespite ($BaFeSi_4O_{10}$), and to other layer silicates. Such a relationship also implied that Cr^{2+} is present in square-planar coordination, making it an interesting candidate for optical absorption spectroscopy. Preliminary details of the $CaCrSi_4O_{10}$ structure refinement have been published as an abstract by Belsky et al. (1981).

Data collection

A single cleavage plate, approximately 120 × 70 × 30 μm was chosen for single crystal precession analysis. Zero- and upper-level photographs taken with Mo$K\alpha$ radiation at 35 kV and 15 mA for 24 to 48 hours exhibited the following systematic absences: hkl: no conditions; $hk0$: $h + k = 2n$; $0kl$: $l = 2n$; and hhl: $l = 2n$. These conditions allow the space group to be chosen as $P4/ncc$ without ambiguity. The minerals gillespite ($BaFeSi_4O_{10}$) and cuprorivaite ($CaCuSi_4O_{10}$) also crystallize in this space group, as do the synthetic compounds $BaMgSi_4O_{10}$, $BaCuSi_4O_{10}$, and $SrCuSi_4O_{10}$ (cited by Mighell et al., 1977).

The crystal fragment was then mounted on a computer-controlled Picker four-circle diffractometer, and intensity data were collected in one octant of reciprocal space from $4° \leq 2\theta \leq 70°$ ($k,k,l \geq 0$). The diffractometer was operated in the constant precision mode using graphite monochromated Mo$K\alpha$ radiation. The total scan width was computed from the formula 2 + 0.7 tan θ(°). A reflection was flagged if $\sigma_I/I > 0.01$, and background counts were measured for a maximum of twenty seconds. All reflection data were corrected for Lorentz and polarization effects during the collection procedure. In all, 2117 reflections (including those that should be absent for space group $P4/ncc$) were collected.

Cell parameters were determined from eight automatically centered reflections using the method of least squares. Final cell parameters for $CaCrSi_4O_{10}$ are **a** = 7.378(5)Å, **c** = 15.119(2)Å, and V = 823.0(6)Å^3, corresponding to a calculated density D (calc.) = 2.941 g/cm^3 with Z = 4. This value is in agreement with the specific gravity D (meas.) = 2.937 g/cm^3, measured by heavy liquid techniques. More precise cell parameters could not be measured, because there are no strong, high-angle general reflections produced by $CaCrSi_4O_{10}$.

Structure refinement

The structure refinement was initiated using the program RADY (Sasaki, pers. comm.), a modification of RADIEL (see Coppens et al., 1979). Atomic coordinates for gillespite (Hazen and Burnham, 1974) were used as initial values. Atomic scattering factor curves for Ca^{2+}, Cr^{2+}, and Si^{4+} were obtained from Ibers and Hamilton (1974), and that for O^{2-} was obtained from Tokonami (1965).

Of the 2117 reflections, 365 were confirmed to obey the systematic absence conditions for the space group $P4/ncc$ and were deleted from the data set. The remaining data were corrected for absorption and the structure refined, followed by an isotropic extinction correction. The data were then averaged and the structure re-refined, converging to R = 0.026 (R_w = 0.031) after four cycles of the final refinement, based on 545 reflections, using an anisotropic thermal model. The observed and calculated structure factors are listed in Table 1.[1]

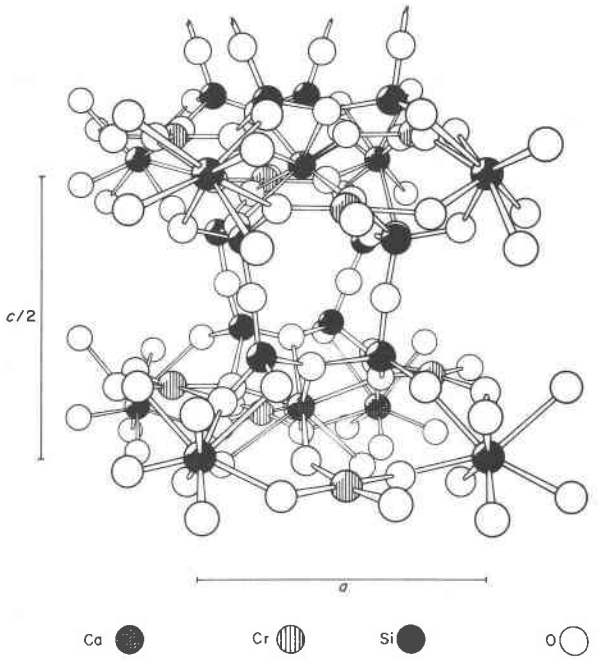

Fig. 1. The crystal structure of $CaCrSi_4O_{10}$.

Discussion of the structure

$CaCrSi_4O_{10}$ (Fig. 1) is a structural analog of gillespite, $BaFeSi_4O_{10}$ (Hazen and Burnham, 1974). As with barium in gillespite, calcium occupies the site with $\bar{4}$ symmetry and is in irregular cubic coordination. Chromium occupies the site with four-fold symmetry and is in nearly ideal square-planar coordination. There are three distinct oxygen atoms in the $CaCrSi_4O_{10}$ structure.

The structure consists of layers of four-member rings of SiO_4 tetrahedra perpendicular to **c**. Each ring is linked to four others by a bridging O1 atom making an Si–O1–Si bond angle of 176.8°. This linking of rings results in an infinite Si_8O_{20} sheet perpendicular to **c**. Each chromium atom, coordinated to four O3 atoms in a nearly square-planar arrangement, lies within a given sheet. Calcium is bonded to four O2 atoms and four O3 atoms in distorted cubic coordination, and serves as a link between upper and lower sheets. The atomic coordinates for $CaCrSi_4O_{10}$ are presented in Table 2, with anisotropic temperature factors listed in Table 3.

[1] To receive a copy of Table 1, order document AM-84-244 from the Business Office, Mineralogical Society of America, 2000 Florida Avenue, N.W., Washington, D. C. 20009. Please remit $5.00 in advance for the microfiche.

Table 2. Atomic coordinates for $CaCrSi_4O_{10}$

Atom	Site	Parameter	Position
Ca	4b	x	0
		y	0
		z	0
Cr	4c	x	0
		y	1/2
		z	0.07951(5)*
Si	16g	x	0.25310(8)
		y	0.17208(7)
		z	0.14801(4)
O1	8f	x	0.20819(25)
		y	0.20819(25)
		z	1/4
O2	16g	x	0.45499(19)
		y	0.24829(22)
		z	0.12833(11)
O3	16g	x	0.10627(20)
		y	0.25049(20)
		z	0.08189(12)

* Parenthesized figures represent the estimated standard deviation (esd) in terms of least units cited for the value to their immediate left.

In the CaO_8 polyhedron, the four Ca–O3 bonds (2.630Å) are shorter than the four Ca–O2 bonds (2.698Å), resulting in a distorted cubic coordination. The shortening of the Ca–O3 bonds is consistent with the fact that O3 is underbonded relative to O2.

In the square-planar group, the chromium atom is only 0.0025Å out of the plane of the four bonding O3 atoms. The Cr–O3 bond distance is 2.000Å, close to the 1.995Å bond distance determined for square-planar Fe^{2+} in gillespite (Hazen and Burnham, 1974).

In the SiO_4 tetrahedra, the average Si–O bond distance is 1.609Å. Again, underbonding of the O3 atom may explain why the Si–O3 bond length (1.581Å) is the shortest, and similar reasoning can be used to explain the relative Si–O2 and Si–O3 bond distances.

The Si–O1–Si bond angle of 176.8° is unusually large, although angles of such magnitude have been reported for gillespite, 177.7° (Hazen and Burnham, 1974), thortveitite

Table 3. Anisotropic temperature factors for $CaCrSi_4O_{10}$

Atom	β_{11}	β_{22}	β_{33}	β_{12}	β_{13}	β_{33}	B_{eq}
Ca	0.00307(3)	0.00307(3)	0.00092(1)	0	0	0	0.725(3)
Cr	0.00171(4)	0.00171(4)	0.00127(4)	0	0	0	0.635(3)
Si	0.00185(3)	0.00189(3)	0.00084(0)	0.00009(2)	0.00003(1)	-0.00006(1)	0.528(5)
O1	0.00809(11)	0.00809(11)	0.00180(10)	-0.00125(13)	0.00068(3)	-0.00068(3)	1.721(12)
O2	0.00168(8)	0.00511(9)	0.00159(1)	-0.00067(8)	-0.00015(2)	0.00050(2)	0.976(15)
O3	0.00262(8)	0.00221(8)	0.00183(1)	0.00049(7)	-0.00059(2)	-0.00005(2)	0.909(14)

Temperature factor is in the form $\exp[-(h^2\beta_{11}+k^2\beta_{22}+l^2\beta_{33}+2hk\beta_{12}+2hl\beta_{13}+2kl\beta_{23})]$

Parenthesized figures represent the estimated standard deviation (esd) in terms of least units cited for the value to their immediate left.

Table 4. Bond distances and angles for $CaCrSi_4O_{10}$

Bond	Distance (Å)	Average (Å)
Ca–O2	2.698(1)*	2.529
Ca–O3	2.360(1)	
Cr–O3	2.000(1)	
Si–O1	1.601(3)	
Si–O2	1.623(1)	1.609
Si–O2	1.629(1)	
Si–O3	1.581(1)	
Si–Si	3.201(1)	3.171
Si–Si	3.140(1)	
Atoms	**Angle (°)**	
O3–Cr–O3	89.98(0)	
O3–Cr–O3	177.90(9)	
Si–O1–Si	176.82(9)	
Si–O1–Si	149.88(10)	
O1–Si–O2	108.19(9)	
O1–Si–O2	110.03(6)	
O1–Si–O3	113.91(10)	
O2–Si–O3	103.73(8)	
O2–Si–O3	112.54(8)	

* Parenthesized figures represent the estimated standard deviation (esd) in terms of least units cited for the value to their immediate left.

180° (Smolin et al., 1973) and coesite, 180° (Araki and Zoltai, 1969; Gibbs, et al., 1977). Liebau (1961) argued that such high-angle bonds are energetically unfavorable, but Gibbs et al. (1981) concluded that only at angles below about 120° are Si–O–Si bonds highly unstable. A summary of bond lengths and bond angles appears in Table 4.

Table 5 lists the magnitude and orientation of the ellipsoids of thermal vibration for each atom. As expected, the O1 atom, bonded only to two cations, shows the

Table 5. Ellipsoids of thermal vibration for $CaCrSi_4O_{10}$

Atom	Axis	RMS displacement (A)	Angle (°) with respect to a	b	c
Ca	1	0.0928	180.00	90.00	90.00
	2	0.0928	180.00	90.00	90.00
	3	0.1034	90.00	90.00	0.00
Cr	1	0.0701	0.00	90.00	90.00
	2	0.0701	180.00	90.00	90.00
	3	0.1140	90.00	90.00	0.00
Si	1	0.0708	34.96	124.13	96.67
	2	0.0746	124.76	144.97	93.84
	3	0.0955	86.71	96.96	7.71
O1	1	0.0946	102.84	77.16	18.32
	2	0.1498	135.00	135.00	90.00
	3	0.1756	47.84	132.16	71.68
O2	1	0.0672	170.24	99.42	92.52
	2	0.1166	83.02	149.73	60.71
	3	0.1434	96.78	61.52	29.42
O3	1	0.0794	135.19	46.82	99.71
	2	0.0918	129.02	136.30	106.52
	3	0.1368	71.54	84.52	160.69

highest degree of displacement, which is in the direction perpendicular to the Si–O1–Si bond. For square-planar Cr^{2+}, the direction of maximum thermal vibration is, as expected, perpendicular to the four bonding O3 atoms.

The theorem of Jahn and Teller predicts that Cr^{2+} will be stabilized in distorted octahedral environments. Such distortions presumably occur in the CrO_6 unit in Cr_2SiO_4 (Scheetz and White, 1972; Belsky et al., 1981). No major distortion of the gillespite-type structure occurs when Cr^{2+} is present, suggesting that Cr^{2+} enters the gillespite structure because the square-planar site is already favorable. This is reasonable because the square-planar environment can be viewed as the limiting case to which an octahedron can be distorted by the elongation of the metal–oxygen bonds along the **c** axis. The square-planar coordination of Cr^{2+} in $CaCrSi_4O_{10}$ is unique among silicate structures, although it has also been reported in the organometallic chromous phthalocyanine (cited by Lever, 1968).

High pressure behavior

A crystal $CaCrSi_4O_{10}$, approximately 80 × 60 × 30 μm, was mounted in a gasketed diamond-anvil pressure cell using a 4:1 methanol:ethanol mixture as the pressure medium. Ruby chips of approximately 10 μm were included for pressure calibration. The crystal was mounted with the **c** axis perpendicular to the flat faces of the diamonds. Crude optical examination revealed a distinct but gradual change in color from magenta to yellow through 25 kbar.

In a continuation of the experiments, an elongated crystal of $CaCrSi_4O_{10}$, approximately 130 × 50 × 40 μm, was mounted for optical and X-ray examination according to the methods outlined above (see Hazen and Finger, 1982).[2] The crystal was mounted with the tetragonal **c** axis parallel to the diamond faces, so that both the ϵ (deep magenta at room conditions and ω (orange at room conditions) optical directions could be observed under a polarizing microscope at high pressure. Between room pressure and 50 kbar, dramatic but gradual color changes were observed in both directions. The ϵ direction changed from deep magenta through red to orange, with a distinct decrease in color intensity over this pressure range. The ω color also shifted to higher energy, from orange to deep yellow at 50 kbar. The changes in pleochroism at high pressure, although striking, are distinct in character from the discontinuous red-to-blue change observed at high pressure in gillespite, which undergoes a first-order phase transition at 18 kbar (Huggins et al., 1976).

A second crystal, approximately 100 × 100 × 40 μm, was mounted in a diamond cell with the **c** axis perpendicular to the flat diamond faces. Unit cell parameters of this crystal were measured at 15.0, 25.9, and 40.3 kbar, as well as at room pressure (all at 24°C), and are listed in Table 6. The crystal remained tetragonal to the highest pressure studied, and changes in cell edges and volume are continuous *versus* pressure. Therefore, a phase transition to an orthorhombic form of $CaCrSi_4O_{10}$, if it occurs, must take place above 40 kbar. Linear compressibility of the **c** axis ($\beta_c = \triangle c/c\triangle P = 6.0 \times 10^{-4}$kbar^{-1}) is more than twice that of the **a** axis ($\beta_a = 2.5 \times 10^{-4}$ kbar^{-1}). This compression behavior is identical to that of gillespite below 18 kbar; in gillespite, $\beta_a = 3.7 \times 10^{-4}$ kbar^{-1}, and $\beta_c = 8.7 \times 10^{-4}$ kbar^{-1}. Thus, the axial compression ratio in both $BaFeSi_4O_{10}$ and $CaCrSi_4O_{10}$ is $\beta_c/\beta_a = 2.4$. It may be assumed therefore, that structural changes in $CaCrSi_4O_{10}$ are similar to those determined by Hazen and Finger (1983) for gillespite. Specifically, the eight-coordinated Ca site, like the Ba site in gillespite, undergoes significant compression, thus primarily reducing the **c** dimension. The square-planar site undergoes moderate compression, comparable to bulk compression in the (001) plane. The silicon tetrahedron undergoes little, if any volume change, although some bending of Si–O–Si angles (in particular, the Si–O1–Si angle) is observed.

The magnitudes of $CaCrSi_4O_{10}$ linear compressibilities are approximately 30% less than in gillespite because of the smaller polyhedral compressibility of calcium compared to barium (Hazen and Finger, 1982). Nevertheless, in all major aspects $CaCrSi_4O_{10}$ below 50 kbar responds to pressure in the same way as gillespite below 18 kbar.

Optical spectroscopy

The optical absorption spectrum of an oriented section of $CaCrSi_4O_{10}$ examined between 300 and 2200 nm shows two prominent absorption bands (Fig. 2). The most intense absorption reaches a maximum at 511 nm for light polarized in (001). Additional structure on the main band occurs at 530, 540, and 551 nm. For light polarized parallel to the **c** axis, an absorption maximum occurs at 453 nm. A broad, weak absorption also occurs centered at ~670 nm in (001). When the sample is at 78 K, the 511 nm absorption becomes sharper, the various components move to slightly shorter wavelengths, the 453 nm band decreases in intensity, but no significant new features are revealed. The intensity of the absorption is moderate; the

Table 6. Unit cell parameters for $CaCrSi_4O_{10}$ at several pressures. (High pressure data were measured by R. M. Hazen, Geophysical Laboratory, Washington, D.C.)

Pressure (kbar)	a (Å)	c (Å)	V (Å^3)
0.001	7.376(2)	15.115(3)	822.3(7)
15.0	7.348(2)	14.961(8)	807.8(10)
25.9	7.327(1)	14.881(8)	798.9(5)
40.3	7.301(2)	14.71(2)	784.5(15)

[2] This phase of the high pressure examination of $CaCrSi_4O_{10}$ was conducted by R. M. Hazen at the Geophysical Laboratory, Washington, D. C.

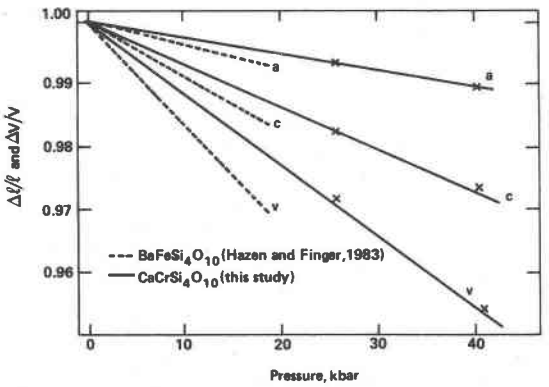

Fig. 2. Linear and volume compression of $CaCrSi_4O_{10}$ and $BaFeSi_4O_{10}$ (gillespite). In both compounds, the c axis is 2.4 times more compressible than the a axis. The barium compound is approximately 50% more compressible than the calcium analog because Ba polyhedra are more compressible than Ca polyhedra.

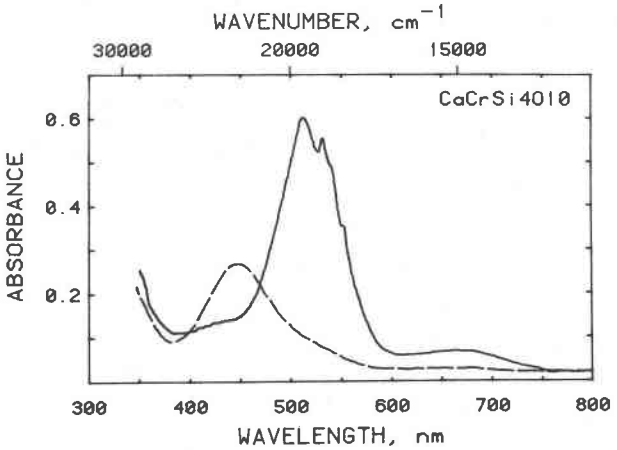

Fig. 3. The 23 °C optical absorption spectrum of an 88 μm thick oriented section of $CaCrSi_4O_{10}$. Solid line $\perp$ **c**; Dashed line $\parallel$ **c**.

ϵ value based on Cr^{2+} is 18 liter/mole · cm for the 511 nm band.

The general appearance of the spectrum is distinct from that of Cr^{3+} in octahedral coordination. No other relevant spectra of Cr^{2+} in square planar coordination are available for comparison. Because of the Jahn–Teller effect, the environment around Cr^{2+} in six-fold coordination may distort to D_{4h} local symmetry by elongation of two axial Cr–O bonds. The spectra of Cr^{2+} in such environments (Clark, 1964; Fackler and Holah, 1965) differs from that of $CaCrSi_4O_{10}$. The spectrum does bear some resemblance to that of Cr_2SiO_4 (Scheetz and White, 1972) which has an absorption maximum near 546 nm with conspicuous structure on the sides.

From the analysis of the spectrum of high spin Cr^{2+} in D_{4h} local symmetry following a procedure similar to that followed by Burns et al. (1966) for gillespite, and by Clark and Burns (1967) for $BaCuSi_4O_{10}$, it can be shown that because purely electronic *d–d* orbital transitions are forbidden, absorption can occur only through vibronic coupling.

Conclusions

The structure of $CaCrSi_4O_{10}$ has been refined to $R = 0.026$ ($R_w = 0.031$) in the space group $P4/ncc$. $CaCrSi_4O_{10}$ is isostructural with gillespite ($BaFeSi_4O_{10}$) and other $ABSi_4O_{10}$ compounds.

The average Si–O bond distance in the SiO_4 tetrahedra is 1.609Å. Summation of Pauling bond strengths can be used to explain the relative lengthening and shortening of the Si–O and Ca–O bonds.

The most interesting aspects of the $CaCrSi_4O_{10}$ structure are (1) the square-planar coordination of Cr^{2+}, and (2) the Si–O–Si bond angle of 176.8°. It appears that Cr^{2+} is stable in the gillespite structure because the square-planar site is already distorted (relative to an octahedron). This is in contrast to other Cr^{2+} compounds in which the structure distorts as a result of the presence of Cr^{2+}. $CaCrSi_4O_{10}$ is the only known silicate that contains square-planar coordinated Cr^{2+}.

Analysis of the spectrum of high spin Cr^{2+} in $CaCrSi_4O_{10}$ examined between 300 and 2200 nm shows that absorption occurs solely through vibronic coupling. Although no other relevant spectra of Cr^{2+} in square-planar coordination are available for comparison, the spectrum does bear some resemblance to that of Cr_2SiO_4.

$CaCrSi_4O_{10}$ remains tetragonal to at least 50 kbar. However, striking changes in pleochroism are observed as pressure is increased. The compression behavior is identical to that of gillespite, suggesting that the structural changes in $CaCrSi_4O_{10}$ are similar to those observed in gillespite.

Acknowledgments

The authors would like to express their thanks to Dr. Satoshi Sasaki and Mr. Ken Baldwin for assistance with X-ray and computer facilities. Figure 1 was expertly drafted by Ms. Lois Koh. Dr. Robert Hazen and Dr. Roger Burns provided critical readings of the manuscript. This research was supported in part by NSF Grant EAR81-20950.

References

Araki, T. and Zoltai, T. (1969) Refinement of a coesite structure. Zeitschrift für Kristallographie, 129, 381–387.

Belsky, H. L., Prewitt, C. T., and Gasparik, T. (1981) The crystal structure of divalent chromium: Structure of $CaCrSi_4O_{10}$. (abstr.) Geological Society of America Abstracts with Programs, 13, 406.

Bunch, T. E. and Fuchs, L. H. (1969) A new mineral: brezinaite, Cr_3S_4, and the Tucson meteorite. American Mineralogist, 54, 1509–1518.

Burns, R. G., Clark, M. C., and Stone, A. J. (1966) Vibronic polarization in the electronic spectra of gillespite, a mineral

containing iron (II) in square-planar coordination. Inorganic Chemistry, 5, 1268–1272.

Clark, M. G. and Burns, R. G. (1967) Electronic spectra of Cu^{2+} and Fe^{2+} square planar coordinated by oxygen in $BaXSi_4O_{10}$. Journal of the Chemical Society A, 1034–1038.

Clark, R. J. H. (1964) Diffuse spectra of some anhydrous transition metal halides. Journal of the Chemical Society, 417–425.

Coppens, P., Guru Row, T. N., Leung, P., Stevens, E. D., Becker, P. J., and Yang, Y. W. (1979) Net atomic charges and molecular dipole moments from spherical-atom X-ray refinements, and the relation between atomic charge and shape. Acta Crystallographica, A35, 63–72.

Fackler, J. P. Jr. and Holah, D. G. (1965) Electronic spectra of chromium (II) complexes. Inorganic Chemistry, 4, 954–958.

Gasparik, T. (1981) Some phase relations involving chromous pyroxenes and other Cr^{2+} bearing phases at pressures less than 1 atmosphere. (abstr.) Proceedings of the Twelfth Lunar and Planetary Science Conference, Part 1, 333–335.

Gibbs, G. V., Meagher, E. P., Newton, M. D., and Swanson, D. K. (1981) A comparison of experimental and theoretical bond length and angle variations for minerals, inorganic solids, and molecules. In M. O'Keeffe and A. Navrotsky, Eds., Structure and Bonding in Crystals, Vol. I, p. 195–225. Academic Press, New York.

Gibbs, G. V., Prewitt, C. T., and Baldwin, K. J. (1977) A study of the structural chemistry of coesite, Zeitschrift für Kristallografie, 145, 108–123.

Haggerty, S. E., Boyd, F. R., Bell, P. M., Finger, L. W., and Bryan, W. B. (1970) Opaque minerals and olivines in lavas and breccias from Mare Tranquillitatis. Proceedings of the Apollo 11 Lunar Science Conference, 1, 513–538.

Hazen, R. M. and Burnham, C. W. (1974) The crystal structures of gillespite I and II: A structure determination at high pressure. American Mineralogist, 59, 1166–1176.

Hazen, R. M. and Finger, L. W. (1982) Comparative Crystal Chemistry. Wiley, New York.

Hazen, R. M. and Finger, L. W. (1983) High-temperature and high-pressure crystallographic study of the gillespite I–II phase transition. American Mineralogist, 68, 595–603.

Huggins, F. E., Mao, H. K., and Virgo, D. (1976) Gillespite at high pressure: results of a detailed Mössbauer study. Carnegie Institution of Washington Yearbook, 75, 756–758.

Ibers, J. A. and Hamilton, W. C. (1974) International Tables for X-ray Crystallography, Vol. IV, Kynoch Press, Birmingham, England.

Keil, K. and Brett, R. (1973) $(Fe,Cr)_{1+x}(Ti,Fe)_2S_4$, a new mineral from the Bustee enstatite achondrite. Meteoritics, 8, 48–49.

Lever, A. B. P. (1968) Inorganic Electronic Spectroscopy. Elsevier Publishing Co., Amsterdam.

Liebau, F. (1961) Untersuchungen über die Grösse des Si–O1–Si Valenzwinkels. Acta Crystallographica, 14, 1103–1109.

Meyer, H. O. A. and Boyd, F. R. (1972) Composition and origin of crystalline inclusions in natural diamonds. Geochimica et Cosmochimica Acta, 37, 2037–2042.

Mighell, A. D., Ondik, H. M., and Molino, B. B. (1977) Crystal data space-group tables. Journal of Physics and Chemistry Reference Data, 6, 675–829.

Scheetz, B. E. and White, W. B. (1972) Synthesis and optical absorption spectra of Cr^{2+}-containing orthosilicates. Contributions to Mineralogy and Petrology, 37, 221–227.

Smolin, Y. I., Shepelev, Y. F., and Titov, A. P. (1973) Refinement of the structure of thortveitite $Sc_2Si_2O_7$. Soviet Physics-Crystallography, 17, 4, 749–750.

Tokonami, M. (1965) Atomic scattering factor for O^{2-}. Acta Crystallographica, 19, 486.

Manuscript received, April 6, 1983;
accepted for publication, January 31, 1984.